Conceptual design of the Radial Gamma Ray Spectrometers system for α particle and runaway electron measurements at ITER

M. Nocente[1,2], M. Tardocchi[2], R. Barnsley[3], L. Bertalot[3], B. Brichard[4], G. Croci[1,2], G. Brolatti[5], L. Di Pace[5], A. Fernandes[6], L. Giacomelli[2], I. Lengar[7], M. Moszynski[8], V. Krasilnikov[3], A. Muraro[1,2], R. C. Pereira[6], E. Perelli Cippo[2], D. Rigamonti[1,2], M. Rebai[1,2], J. Rzadkiewicz[8], P. Santosh[3], J. Sousa[6], I. Zychor[8] and G. Gorini[1,2]

[1]Dipartimento di Fisica "G. Occhialini", Università di Milano-Bicocca, Milano, Italy
[2]Istituto di Fisica del Plasma, Consiglio Nazionale delle Ricerche, Milano, Italy
[3]ITER organization, St Paul Lez Durance Cedex, France
[4]Fusion for Energy, Barcellona, Spain
[5]ENEA C. R. Frascati, Dipartimento FSN, Frascati, Italy
[6]Instituto de Plasmas e Fusão Nuclear, Instituto Superior Técnico, Universidade de Lisboa, 1049-001 Lisboa, Portugal
[7]Jozef Stefan Institute, Ljubljana, Slovenia
[8]National Center for Nuclear Research, NCBJ, Swierk, Warsaw, Poland

Corresponding Author: massimo.nocente@mib.infn.it

Abstract:
The Radial Gamma Ray Spectrometers (RGRS) system is been designed at a conceptual level for alpha particle and runaway electron measurements at ITER and is here described. The system benefits from the most recent advances on gamma-ray spectrometry for tokamak plasmas and combines space and high energy resolution in a single device. We find that RGRS as designed can provide information on α particles on a time scale of 1/10 of the slowing down time for the ITER 500 MW full power DT scenario. In case of disruptions with a typical duration of 100 ms, a time resolution of at least 10 ms for runaway electron studies can be achieved depending on the scenario at the different mitigation levels and beam currents we have simulated.

1 Introduction

The ITER project aims at demonstrating fusion power production with a gain of ten and for a duration of about 400 s when the discharge is driven by the Ohmic transformer. On the path towards this highly ambitious goal, ITER will explore, for the first time, the physics of a burning plasma, i.e. a regime where the heating fraction due to the alpha particles exceeds that of the external auxiliary heating systems. Besides, it will also show that plasma operations at unprecedented high performance can be conducted in a reliable and safe way, for example by avoiding damage of the machine first wall due to the generation of an uncontrolled beam of runaway electrons. The design of a system that can simultaneously be used to measure α particles and runaway electrons is thus instrumental to the very core of the ITER mission. The observation of spontaneous gamma-ray emission from reactions between confined fast ions, such as α particles,

and impurities is the natural way to probe probe the energy distribution and spatial profile of the energetic ions [1, 2]. On the other hand, bremsstrahlung emission induced by confined or deconfined runaway electrons can be used to understand their energy distribution and birth/losses in the different phases of the plasma discharge [3]. As both emissions occur in the MeV range, a single, well calibrated system of gamma-ray spectrometers can be in principle used to fulfil both highly important tasks.
In this proceeding paper we present the conceptual design of the Radial Gamma-Ray Spectrometer (RGRS) system for ITER. The system consists of a set of gamma-ray spectrometers and carefully collimated, radial lines of sight designed for installation in a few of the channels of the Radial Neutron Camera (RNC) system for neutron emission profile measurements at ITER [4]. The paper is organised as follows. General information about gamma-ray measurements and their use in present day tokamaks is briefly summarised in sections 2 and 3. Section 4 presents the results of the calculations of gamma-ray emission from α particles and the related challenges and solutions that have been adopted for ITER. The RGRS detector specifications defined by requirements on α particle studies are then used to determine the capability of the system to also measure runaway electrons in disruptions at currents from 100 kA to 10 MA in section 5. Section 6 summarises our findings.

2 Role of γ ray measurements at ITER

Gamma-ray measurements at ITER have primarily two aims. The first is to measure the profile and energy distribution of α particles born from deuterium-tritium (DT) reactions. This is obtained by observations of the 4.44 MeV gamma-ray emission from the $^9\mathrm{Be}(\alpha, \mathrm{n}\gamma)^{12}\mathrm{C}$ reaction that naturally occurs in the plasma between fusion born α particles and $^9\mathrm{Be}$ impurities. The latter come from the erosion of the machine first wall and are found in the plasma at typical concentrations around 1%. 4.44 MeV gamma-ray emission can in principle provide information on the α particle profile and energy distribution [1] and is therefore of key importance. The detection of 4.44 MeV gamma-rays is obtained by observation of the intensity and shape of the full energy peak in the pulse height spectrum resulting from the interaction of the radiation with the spectrometer [5, 6].
The second goal of gamma-ray measurements at ITER is the detection and study of runaway electrons (REs). Gamma-rays are in this case generated from bremsstrahlung emission and carry information on the energy distribution and current of the REs [3]. Unlike gamma-rays from the $^9\mathrm{Be}(\alpha, \mathrm{n}\gamma)^{12}\mathrm{C}$ reaction with a well defined energy (4.44 MeV), the bremsstrahlung process generates radiation with a continuous energy spectrum (see section 5) and that mostly interacts with the detector via Compton scattering. It is therefore the whole shape of the gamma-ray emission spectrum - and not only a narrow energy band - that is of relevance for RE studies with gamma-ray spectrometers.

3 State of the art and main RGRS features

The most advanced set of gamma-ray spectrometers to date is installed at the Joint European Torus (JET) tokamak. In order to obtain spatial and energy information on the energetic particles responsible for gamma-ray emission, two separated systems exist:

a) a set of large (3”x6”, diameter x height), high resolution spectrometers [7], which are

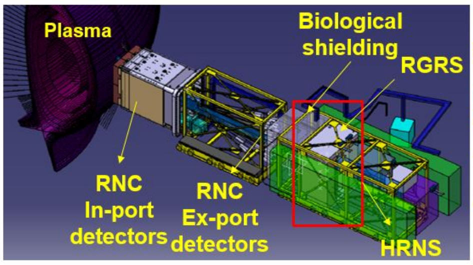

FIG. 1: Schematics of the RGRS position with respect to the Radial Neutron Camera (RNC), the High Resolution Neutron Spectrometer (HRNS) and ITER plasmas.

installed along one vertical and one horizontal lines of sight. The most advanced spectrometers used at JET are $LaBr_3$ and high purity Germanium (HpGe).

b) a gamma-ray camera [1], i.e. a set of detectors at the end of collimated lines of sight which are used to determine the map of the gamma-ray emission in the poloidal plane by tomographic inversion.

As gamma-ray diagnostics were not integrated in the initial JET design, large detectors at sufficiently high energy resolution to allow for measurements of the peak shape broadening along each channel of the gamma-ray camera cannot be developed, due to space limitation. For this reason, at JET, profile and energy distribution measurements are accomplished by two *separate* systems, the camera and the high resolution detectors, respectively.
Contrary to JET, ITER has a larger volume and the RGRS system is being designed in a integrated way with the RNC. Therefore, a system that combines space and energy distribution measurements of the energetic particles can be devised by displacing high resolution detectors in a camera assembly. This is the main principle behind the RGRS design.
The location of the system, as well as the number of lines of sight available, were determined by interfacing constraints with the RNC. These have resulted in the location of the system shown in figure 1, where RGRS is found between the biological shielding and the high resolution neutron spectrometer (HRNS). RGRS has up to 8 radial sightlines shared with the RNC. In terms of spatial coverage in the poloidal plane, this is limited to a radial region $r < a/3$, where $a = 2$ m is the machine minor radius. The radial limitation comes from the unavailability of the RNC in-port lines of sight for RGRS.

4 Alpha particle studies with RGRS

4.1 Modelling

In order to determine the capability of RGRS to study α particles in ITER DT plasmas, we have calculated the expected signal at 4.44 MeV from the $^9\mathrm{Be}(\alpha, \mathrm{n}\gamma)^{12}\mathrm{C}$ reaction for the full power 500 MW ITER scenario using a semi-analytical approach. Plasma parameters were taken from [8] and a ^{9}Be concentration of 1% was assumed. The GENESIS code [9, 6] was used to evaluate the local gamma-ray emissivity $y_\gamma(r, z)$ $[\gamma \cdot \mathrm{s}^{-1} \cdot \mathrm{m}^{-3}]$ at each (r, z) position of the poloidal cross section. This resulted in the map of figure 2, where 4.44 MeV gamma-ray emission is compared to that from fusion born 14 MeV neutrons. The comparison shows that the plasma produces about 40000 neutrons per 4.44 MeV gamma-ray, which requires to use suitable attenuators, see

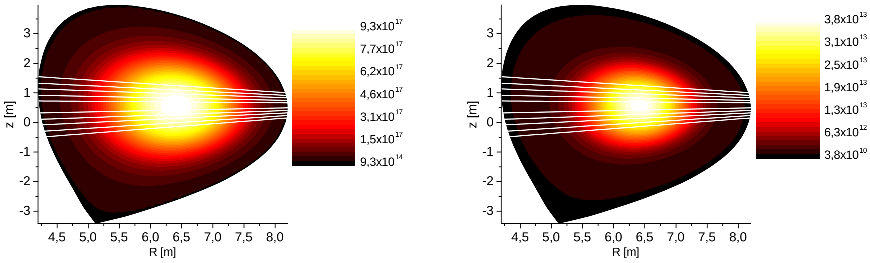

FIG. 2: Calculated 14 MeV neutron (left) and 4.44 MeV γ-ray (right) emissivities (particles/m^3*/s) in the poloidal plane for the ITER 500 MW DT scenario. White lines indicate the RGRS observation chords.*

the next paragraph.
From the local neutron or gamma-ray emissivity $y_{n,\gamma}(r,z)$, and assuming narrow sight-lines, the flux $\phi[\gamma \cdot \mathrm{s}^{-1} \cdot \mathrm{cm}^{-2}]$ impinging on each detector of the RGRS system is estimated by [10]

$$\phi_{n,\gamma} = \frac{1}{16}\left(\frac{d_C}{L}\right)^2 \int_\lambda y_{n,\gamma}(s)ds \tag{1}$$

where λ is the line of sight, d_C is the collimator diameter and L its length. The counting rate r at the detector is finally given by

$$r_{n,\gamma} = \phi \cdot \pi/4 \cdot d_c^2 \epsilon \tag{2}$$

where ϵ is here either the detector full peak efficiency at 4.44 MeV, or the 14 MeV neutron detector efficiency of $LaBr_3$ [11]. The subscripts n and γ in equation 2 indicate neutrons and gammas, respectively. By combining equations 1 and 2 is it seen that r scales as d_C^4.
Detailed MCNP simulations show that equations 2 and 1 provide an accuracy between 20% and 30% with respect to a detailed transport model. This is well within the uncertainty on simulated plasma parameters for the ITER DT scenario and validates our simplified, semi-analytical approach.

4.2 Detector solutions and interfacing issues

From equations 1 and 2 the expected counting rate depends on L, d_C and ϵ, which are set by the collimator (L and d_c) and the detector choice (ϵ). The upper limit on ϵ is determined by the largest, high resolution scintillator crystal presently available, which is the 3"x6" $LaBr_3$ installed at JET and this is also adopted for RGRS. For this detector, we obtain $\epsilon \approx 20\%$. The RNC design sets $L=$ 3 m, while d_C can be (at most) of a few cm. If we use d_C=4 cm and assume to exploit all of the flux impinging at the RNC position, we obtain $r_\gamma \approx$120 kHz in the central channel of RGRS if no attenuation occurs along the line of sight. However, we also correspondingly find $r_n \approx 2.4 \cdot 10^{10}$ Hz given that $\epsilon \approx 1$ for the detection of 14 MeV neutrons by $LaBr_3$ [11]. This counting rate would paralyse the detector and make any measurement impossible. In order to overcome the strong imbalance between r_γ and r_n, the RGRS design includes the use of LiH[12] as attenuator in front of each detector. MCNP simulations have been carried out and revealed that a 120 cm LiH sample provides an attenuation factor of 10^6 to 14 MeV neutrons with a modest reduction of ≈ 10 for the gamma-ray flux. When this is included in

the RGRS model, we find $r_\gamma \approx 12$ kHz (and an overall detector load from 4.44 MeV gamma-rays of 60 kHz). For comparison, $r_n \approx 10$ kHz. This background is however spectrally distributed mostly at $E_\gamma < 3$ MeV and only about 40 Hz falls in the region of the 4.44 MeV peak. The background induced by direct 14 MeV neutrons is therefore negligible after the attenuators.
Full MCNP simulations reveal that the main limitation to the signal-to-background (S/B) ratio comes instead from the generation of background gamma-rays from the capture of 14 MeV neutrons as they cross the LiH attenuator and thermalize in the collimator inside the bio-shielding. A preliminary calculation gives $S/B \approx 3$ at the 4.44 MeV peak. The same calculation shows that the effect of background neutrons and gamma-rays coming from radiation leakage outside the collimators can be completely suppressed by a carefully designed shielding. As spatial information on the α particles resides in the intensity of the 4.44 MeV peak measured by the different detectors, with $S/B \approx 3$ and $r_\gamma \approx 12$ kHz we find that an integration time of 25 ms is required to determine the intensity of the 4.44 MeV emission with an accuracy of 10%. For spectral measurement of the peak broadening we set to have at least 1000 counts in the full energy peak of the detector located in the central channel of RGRS, net of background, which we can achieve in about 0.13 s. Both numbers show that an RGRS system with 3"x6" $LaBr_3$ detectors, 120 cm LiH attenuators, d_C= 4 cm and the lines of sight shown in figure 2 can be integrated with the RNC and combines spatial and energy distribution measurements of α particles with a time resolution of the order of 1/10 of the α particle slowing down time for the 500 MW DT ITER scenario. Here we note that the time resolution is significantly affected by the collimator diameter, as it depends on d_C^4 (see equation 2). For example, if d_C had to be reduced to 2.5 cm for engineering reasons, the integration time to reach the same statistics would correspondingly be increased to $(4/2.5)^4 \approx 6.6$. This gives about 0.16 s and 0.85 s for space and energy information on the α particles, respectively.
As the overall detector load is limited to < 100 kHz, we also note that an HpGe detector can be used to improve the energy resolution of the measurement by a factor > 10, albeit with a 5 time reduced detector efficiency and a correspondingly longer integration time to achieve the same statistics. In our design, we devise to use both an HpGe and $LaBr_3$ detectors for the central channel of RGRS, where the selection between the two is done by means of a slider such as at JET.

5 Runaway electron studies with RGRS

5.1 Hard x-ray emission from runaway electrons

The performance of RGRS as determined by the need to measure α particles at ITER has been also evaluated against runaway electron measurements. To this end, we have extended the GENESIS code so to simulate thin target bremsstrahlung emission from confined runaways with arbitrary spatial and energy distributions at ITER.
The double differential cross section for the production of a gamma-ray at energy W by an electron of energy E, at an angle θ_V between the RE velocity and the emission and per unit solid-angle Ω can be written as [14]

$$\frac{d^2\sigma}{dW d\Omega} = \frac{d\sigma}{dW}\frac{1}{2\pi}p(Z, E, k, \cos\theta_V) \tag{3}$$

where Z is the atomic number of the target bremsstrahlung impurity and $k = W/E$. $d\sigma/dW$ indicates the energy-loss differential cross section, which is described in GENESIS by a modified

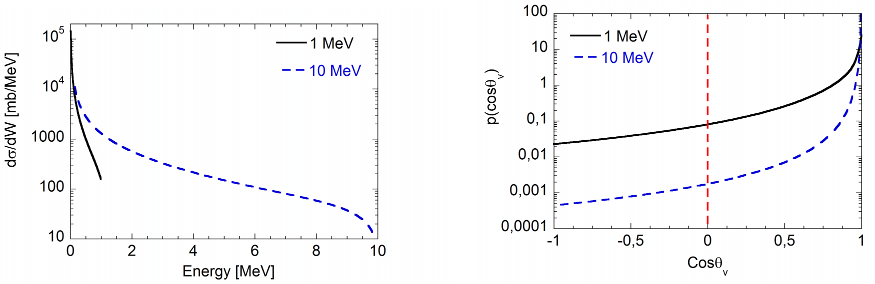

FIG. 3: (left) Differential cross section for the production of gamma-rays as a function of the gamma-ray energy (right) Angular probability of gamma-ray emission as a function of the cosine of the angle between the line of observation and the runaway electron velocity. Results are shown for 1 and 10 MeV runaway electrons. The red dashed line indicates the angle of observation of the RGRS system.

Bethe-Heitler formula according to equation (49) of [13]. The main difference with respect to the pure Bethe-Heitler cross section is the inclusion of a high energy Coulomb and low energy empirical corrections.
$p(Z, E, k, \cos\theta_V)$ is the probability distribution function of $\cos\theta_V$ and is described by a dipole distribution in the rest frame of the runaway electron (see equation (25) of [14]). Compared to the most advanced models of bremsstrahlung emission available to date [14], equation 3 with the mentioned prescriptions for $d\sigma/dW$ and $p(Z, E, k, \cos\theta)$ is somewhat less accurate at $E < 1$ MeV, which is however of little relevance for ITER applications (see below).
Figure 3 shows an example of $d\sigma/dW$ and $p(Z, E, k, \cos\theta)$ for E =1 and 10 MeV REs. Here we note that, as expected, the bremsstrahlung cross section is larger by $10^4 - 10^5$ times at $k << 1$ with respect to $k \approx 1$. The emission is mostly along the direction of the RE velocity and is decreased by 4-5 orders of magnitude for $\cos\theta_V \approx 0$, which is the emission angle of relevance for RGRS when bremsstrahlung radiation is produced by the strongly passing REs.

5.2 Diagnostic capabilities

We have performed a first evaluation of the signal from confined REs expected at RGRS for a hypothetical disruption scenario when the runaway current is I_{RE} =10 MA. We assume an exponential runaway electron distribution of strongly passing (pitch=1) REs with mean energy 12.5 MeV and minor radius of 1 m for the RE beam [15]. Here we consider the case of an unmitigated and mitigated disruptions, with details given in table I.
Figure 4 shows the bremsstrahlung spectrum emitted from a point at the centre of RE beam and when the radiation is towards the RGRS detectors. The mean spectral energy $< E_\gamma >$ is about 100 keV. By evaluating the counting rates at RGRS for all scenarios with equation 2 we find that they are always above 1 MHz (see table I). Considering that at $< E_\gamma >$=100 keV we can operate $LaBr_3$ up to an upper limit of 10 MHz, we find that RGRS can cope with the emission from a I_{RE} =10 MA RE beam in all scenarios but for the large injection case. On the other hand, as the counting rate scales linearly with I_{RE}, RGRS can guarantee a time resolution of 10 ms in at least one of three scenarios of table I and at any value of I_{RE} between 100 kA to 10 MA. The time resolution is here evaluated as the integration time required to detect at least 10^4 events in the spectrum. This is deemed sufficient to determine the RE energy distribution and

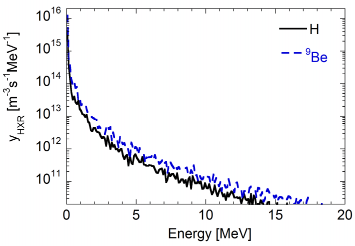

FIG. 4: Simulated gamma-ray emission spectrum impinging on the RGRS system at ITER from runaway electrons in a non mitigated disruption when the runaway current is 10 MA. The y axis indicates the emissivity in the plasma center for gamma-rays emitted towards the RGRS detectors. The bremsstrahlung emission spectrum from collisions with hydrogen and ^{9}Be is separately shown.

TABLE I: Disruption scenarios and results on the counting rate expected at the RGRS detectors as simulated with the GENESIS code. Small and large injection refer to a disruption scenario that is mitigated by the introduction of impurities in the plasma.

Scenario	Impurity species	Impurity density (10^{20} m^{-3})	Hydrogen density (10^{20} m^{-3})	Counting rate [Hz] ($E_\gamma > 500$ keV)
Unmitigated	Beryllium	0.1	0.5	$2.5 \cdot 10^6$
Small injection	Neon	0.05	1.0	$6.4 \cdot 10^6$
Large injection	Neon	25.0	0.5	$2.4 \cdot 10^8$

current with the deconvolution methods of reference [3]. For comparison, the overall duration of a disruption at ITER is about 100 ms.

6 Outlook and conclusions

The Radial Gamma Ray Spectrometers (RGRS) system is being designed for alpha particle and runaway electron (RE) measurements at ITER. By combining the most advanced detector solutions available for tokamak plasmas, RGRS can combine space and energy distribution measurements of α particles and REs in a single system. With our design choices, we are capable to provide α particle measurements by detection of the associated 4.44 MeV gamma-ray emission on a time scale of the order of 1/10 of the α particle slowing down time for the 500 MW full power DT phase of ITER. The performance of the system against runaway electron measurements has also been assessed for a disruption scenario with runaway electron currents between 100 kA and 10 MA. We find that a time resolution of 10 ms can be achieved in at least one of the mitigation scenarios we have considered at any RE current. This compares to an expected duration of the disruption of 100 ms. Based on these encouraging results, a full performance assessment of the system is ongoing with respect to its detailed sensitivity to the α particle and RE velocity space, including a more precise evaluation of the signal-to-background ratio. A detailed engineering model of the system is also being prepared.

References

[1] KIPTILY, V.G. et al. Plasma Phys. Control. Fusion 48 (2006) R59-R82

[2] TARDOCCHI M. et al. Plasma Phys. Control. Fusion 55 (2013) 074014

[3] SHEVELEV A.E. et al. Nucl. Fusion 53 (2013) 123004

[4] MAROCCO D. et al. "System Level Design and Performances of the ITER Radial Neutron Camera", These Proceedings

[5] NOCENTE M. et al. Nucl. Fusion 52 (2012) 063009

[6] TARDOCCHI M. et al. Phys. Rev. Letters 107 (2011) 205002

[7] NOCENTE M. et al. Rev. Sci. Instrum. 81 (2010) 10D321

[8] POLEVOI A., "Assessment of Neutron Emission from DD to DT operation of ITER", IDM UID Q43JH7

[9] NOCENTE M., PhD Thesis, https://boa.unimib.it/handle/10281/28397 (2012)

[10] BATISTONI P. et al. Rev. Sci. Instrum. 66 (1995) 4949

[11] CAZZANIGA C. et al. Nucl. Instrum. Meth. A 778 (2015) 20

[12] CHUGUNOV I. et al. Instruments and Experimental Techniques 51 (2008) 166

[13] SALVAT F et al. Radiation Physics and Chemistry 75 (2006) 1201

[14] SALVAT F. and FERNANDEZ-VAREA J.M. Nucl. Instrum. Meth. B 63 (1992) 255

[15] LEHNEN M. Private Communication